Supporting Information

Designed synthesis of prussian blue@Cu-doped zinc phosphate nanocomposites for chemo/chemodynamic/photothermal combined cancer therapy

Xiaoxue Hu[a], Xiaoning Song[a], Yuan Yuan[a], Xintao Yao[a], Xiangjun Chen[b], Gang Li*[a], Shengnan Li*[a]

[a]School of Chemical Engineering and Technology, Hebei University of Technology, Xiping Road, Tianjin 300401, P. R. China.

[b]School of Pharmacy, Shandong New Drug Loading & Release Technology and Preparation Engineering Laboratory, Binzhou Medical University, 346 Guanhai Road, Yantai 264003, P. R. China.

Email: lisn027@hebut.edu.cn

Materials: potassium ferricyanide, zinc oxide, and doxorubicin hydrochloride (DOX) were purchased from Shanghai Macklin Biochemical Co. Ltd and polyacrylic acid (PAA) was obtained from Sigma-Aldrich. Copper chloride dihydrate, ammonium dihydrogen phosphate, reduced glutathione (GSH), 5,5'-dithiobis-(2-nitrobenzoic acid) (DTNB), and polyvinylpyrrolidone (PVP) came from Shanghai Aladdin Biochemical Technology Co. Ltd. Live-Dead Cell Staining Kit and 2',7'-Dichlorodihydrofluorescein diacetate (DCFH-DA) were received from Beyotime Biotechnology. All reagents were used after receiving and without further purification.

Characterization: the PB@Cu^{2+}/ZnP NPs were performed by Transmission electron micrographs (TEM, FEI Talos F200S), Scanning electron microscopy (SEM, FEI Nova Nano SEM 450), X-ray diffractometer (XRD, Bruker D8) and X-ray photoelectron spectroscopy (XPS, Thermo ESCALAB 250Xi). The UV-vis absorbance spectra were measured by a spectrometer (TU-1810 SPC). Hydrated size distribution detected by dynamic light scattering (DLS) (Malvern, Zetasizer Nano ZS-90). Specific surface area and pore size distribution were investigated by ASAP 2460 and the pore size was calculated by the N_2 absorption-desorption isothermal method.

Cellular uptake: Cellular uptake of PB@Cu^{2+}/ZnP NPs were assessed by CLSM and flow cytometric analysis. HepG-2 cells and PB@Cu^{2+}/ZnP NPs were incubated in a 6-well plate (density: 2×10^5 per well) for 3 h at 37 °C. After that, wash 3 times with PBS and then be stained with DAPI for 30 min. Eventually, the treated cells were monitored by laser confocal microscopy. Flow cytometry analysis was further analyzed. HepG-2 cells were cultured in 6-well plates for different periods of time. The cells were collected and analyzed by flow cytometry analysis.

In vitro synergistic treatment: The cytotoxicity of the PB@Cu^{2+}/ZnP NPs by using HepG-2 cells were evaluated by standard MTT assay. HepG-2 cells were plated in 96-well plates and cultured with different concentrations of PB@Cu^{2+}/ZnP NPs, PB@Cu^{2+}/ZnP NPs + DOX, PB@Cu^{2+}/ZnP NPs + laser, and PB@Cu^{2+}/ZnP NPs + DOX + laser treated for 24 h. After this, MTT solution was inserted into each well and then incubated for 4 h. After that 200 μL of DMSO was added and incubated for another

10 min on a shaker. Finally, the absorbance at 490 nm was obtained by placing the 96-well plate in a microplate reader and relative cell viability was calculated from the absorbance of each well.

Cell viability was also measured using a Live/Dead cell staining assay. In brief, HepG-2 cells were cultured overnight in 6-well plates and were incubated in different treatments for 6 h. After washing three times with PBS, the obtained cells were stained with Calcein-AM and PI solution for 15 min and then observed with CLSM.

In vivo NIR imaging: The mice were treated with PBS and PB@Cu^{2+}/ZnP NPs, irradiated with 808 nm laser for 10 min after 24 h, and then infrared imaging images were taken at different times at the tumor site.

H&E stained: Mice were executed after 11 d of treatment, and the major organs (heart, liver, spleen, lung, and kidney) and tumor tissues from different treatment groups were removed, dehydrated in formalin, ethanol, and xylene buffer, made into paraffin sections and cut into 3 × 5 mm^2 sections. Then, the tissue sections were stained with H&E to enable observation under a fluorescence inverted microscope.

Statistical analysis: The error of parallel test was calculated as mean ± SD. Statistical difference was calculated through two-tailed t-test. Asterisks indicated significant differences (*$P < 0.05$, **$P < 0.01$, ***$P< 0.001$). *$P < 0.05$ was considered to be statistically significant.

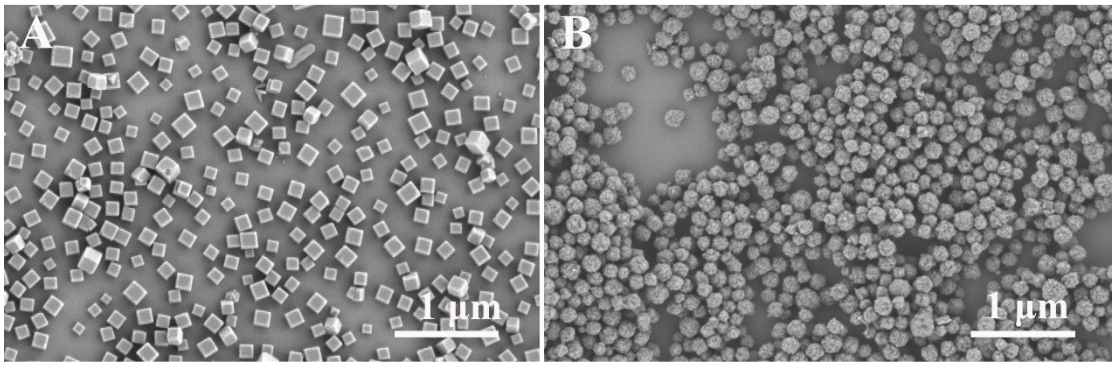

Figure S1. SEM images of (A) PB NPs and (B) PB@Cu^{2+}/ZnP NPs.

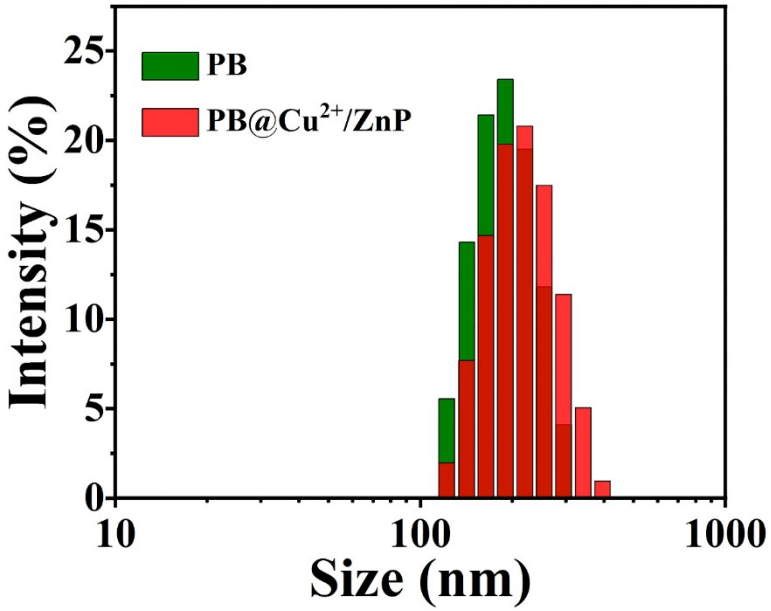

Figure S2. Size distribution of PB NPs and PB@Cu^{2+}/ZnP NPs.

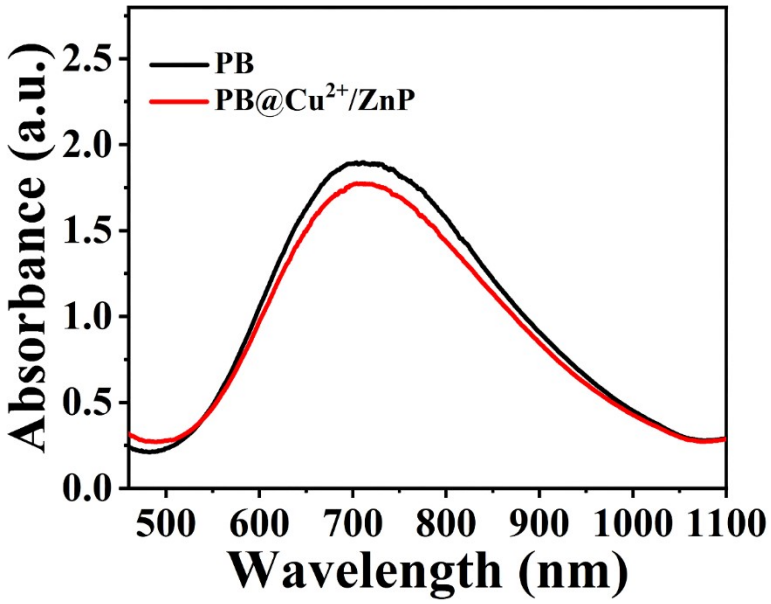

Figure S3. UV-vis-NIR spectra of PB NPs and PB@Cu^{2+}/ZnP NPs.

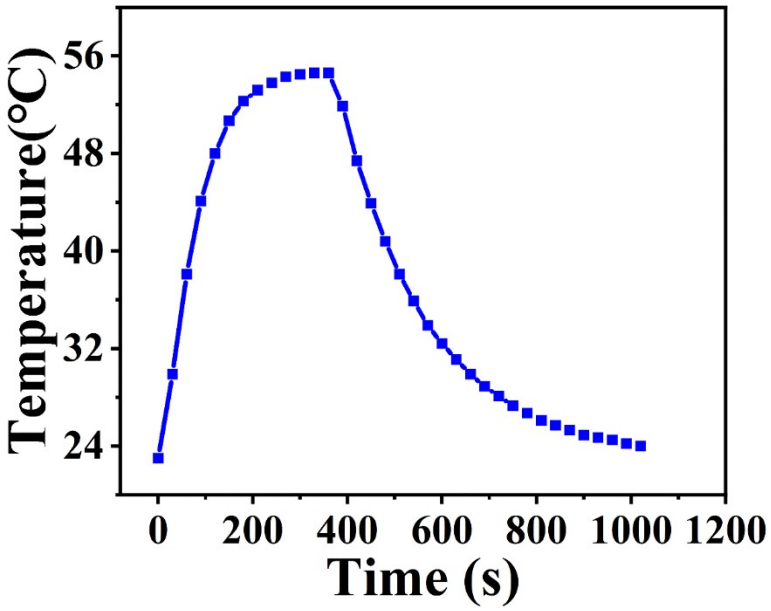

Figure S4. Temperature curve of PB@Cu^{2+}/ZnP NPs with laser on/off.

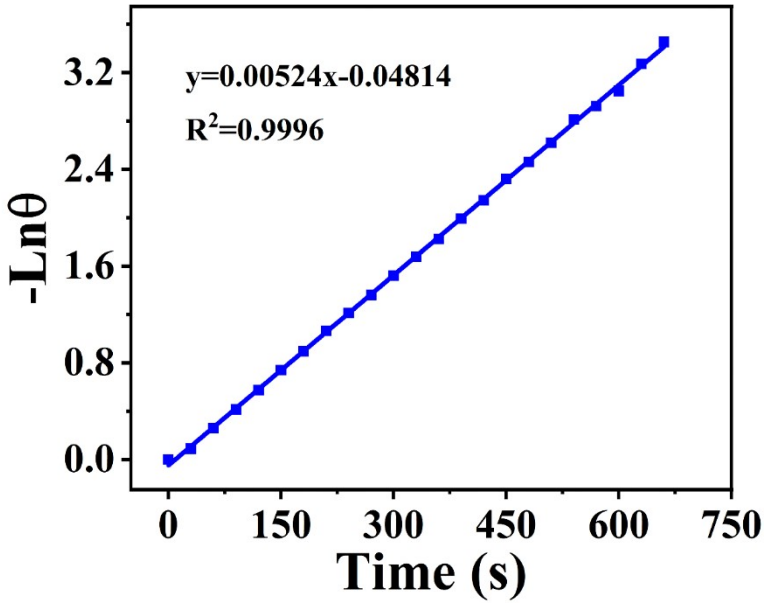

Figure S5. Fitted curve of photothermal conversion efficiency of PB@Cu^{2+}/ZnP NPs.

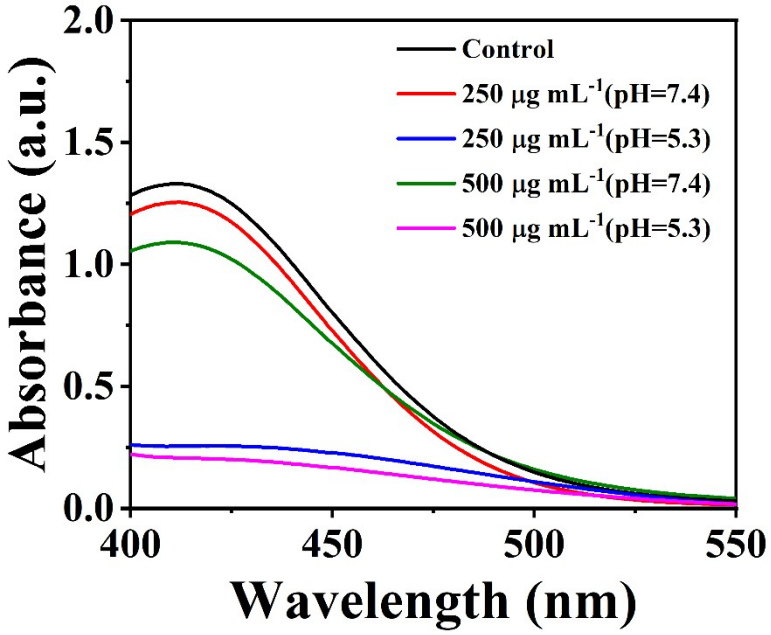

Figure S6. GSH depletion at different pH.

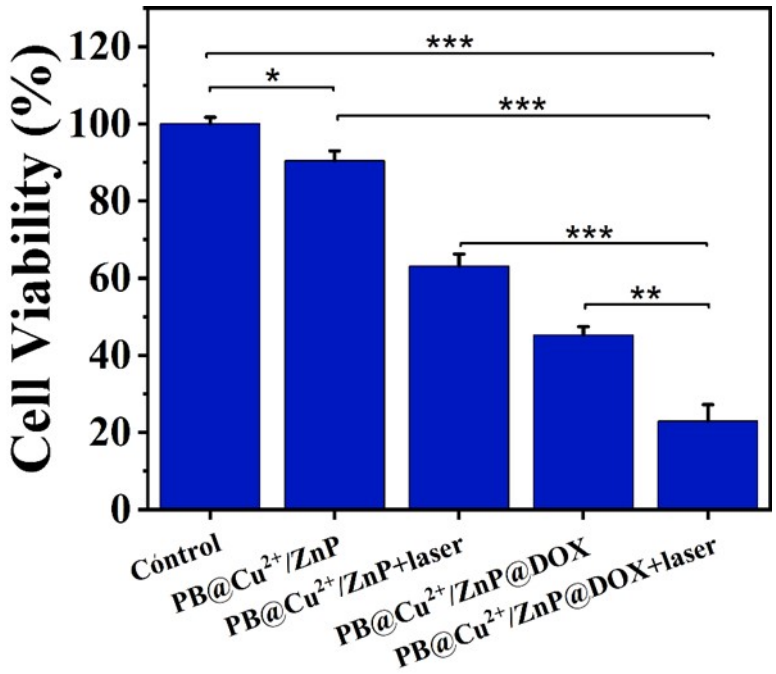

Figure S7. Relative viabilities of HepG-2 cells after various treatments.

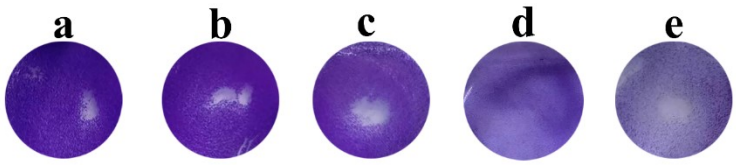

Figure S8. Crystal Violet-stained images of HepG-2 cells with various treatments. a: control, b: PB@Cu^{2+}/ZnP NPs, c: PB@Cu^{2+}/ZnP NPs + laser, d: PB@Cu^{2+}/ZnP@DOX NPs, e: PB@Cu^{2+}/ZnP@DOX NPs + laser.

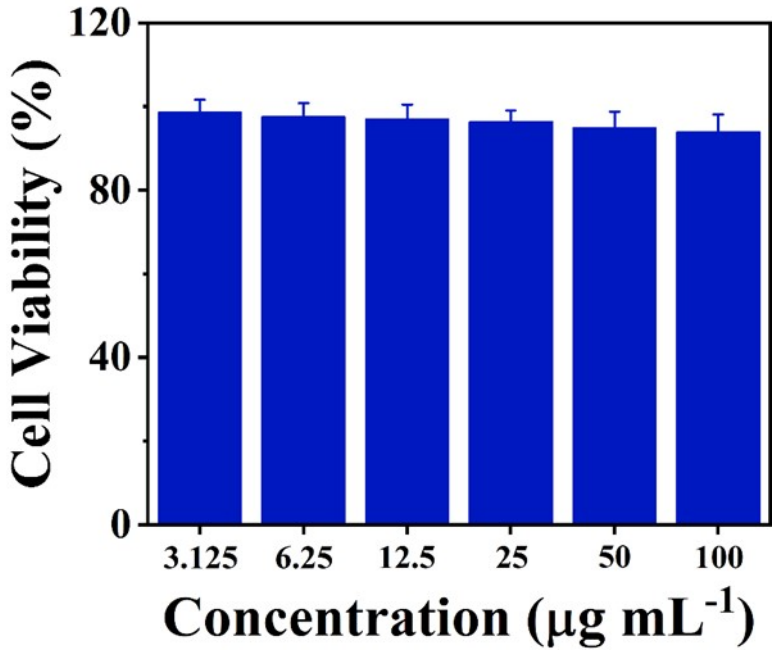

Figure S9. Relative viabilities of 293T cells treated with PB@Cu^{2+}/ZnP NPs.

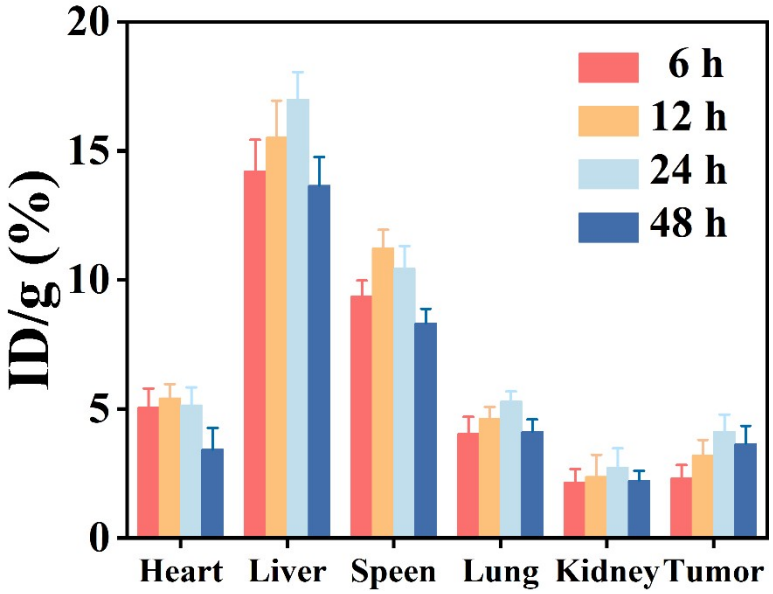

Figure S10. In *vivo* bio-distribution of PB@Cu^{2+}/ZnP at different post-injection time by measuring Fe content.